

## RADIOCARBON DATING OF LEAF WAXES IN THE LOESS-PALEOSOL SEQUENCE KURTAK, CENTRAL SIBERIA

Mischa Haas<sup>1,2\*</sup> • Marcel Bliedtner<sup>3</sup> • Igor Borodynkin<sup>4</sup> • Gary Salazar<sup>5</sup> •  
Sönke Szidat<sup>5</sup> • Timothy Ian Eglinton<sup>2</sup> • Roland Zech<sup>3</sup>

<sup>1</sup>Swiss Federal Institute of Aquatic Science and Technology (Eawag), 8600 Dübendorf, Switzerland.

<sup>2</sup>Department of Earth Sciences, ETH Zürich, 8092 Zürich, Switzerland.

<sup>3</sup>Geographical Institute and Oeschger Centre for Climate Change Research, University of Bern, 3012 Bern, Switzerland.

<sup>4</sup>Krasnoyarsk State Pedagogical University, 660060 Krasnoyarsk, Russia.

<sup>5</sup>Department of Chemistry & Biochemistry and Oeschger Centre for Climate Change Research, University of Bern, 3012 Bern, Switzerland.

**ABSTRACT.** Loess-paleosol sequences (LPS) are valuable archives for Quaternary climate and environmental changes. So far, LPS are generally dated using luminescence, with ~10% uncertainties, or radiocarbon (<sup>14</sup>C) analyses in the rare cases that charcoal or macrofossils are available. For this study, we determined <sup>14</sup>C ages of leaf waxes (long-chain *n*-alkanes) extracted from the LPS Kurtak in central Siberia. <sup>14</sup>C ages range from 16.7 to 22.9 ka cal BP for the last glacial loess and from 24.5 to 35.3 ka cal BP for the paleosol correlated with marine isotope stage (MIS) 3. Overall, this is in good agreement with independent age control based on stratigraphy, infrared stimulated luminescence (IRSL) dating, and <sup>14</sup>C dating on charcoal and macrofossils. However, strong cryoturbation and solifluction seem to have affected the MIS 3 paleosol early during MIS 2. Our results corroborate the stratigraphic integrity of leaf waxes, and highlight their potential for dating LPS back to ~35–40 ka BP. Compared to compound-specific <sup>14</sup>C analyses, which are very time-consuming and require specialized instrumentation (gas chromatograph with fraction collector), <sup>14</sup>C dating of leaf waxes as a whole compound class is relatively quick and straightforward and warrants further investigation as a chronological tool.

**KEYWORDS:** loess-paleosol sequences, EA-AMS <sup>14</sup>C dating, long-chained *n*-alkanes, central Siberia, leaf waxes.

### INTRODUCTION

Ice cores, marine and lake sediments provide important insights into past climate changes, and much of our knowledge concerning Quaternary climate history, as well as mechanisms and forcing of climate change, comes from those archives (Bradley 1999). Loess-paleosol sequences (LPS) are valuable terrestrial archives, which are important in order to refine climate reconstructions regionally and to understand environmental consequences of climate change, both in the geologic past and the future (Field and Van Aalst 2014). LPS form due to eolian transport and deposition of mineral dust and record more or less favorable conditions for pedogenesis in the past (Pécsi 1990). It has, for example, long been recognized that the more than 200-m-thick LPS on the Chinese Loess Plateau reflects the alternation of cold and dry glacials with warm and more humid interglacials during the Quaternary (Kukla 1987; Derbyshire et al. 1997). Extensive LPS also occur in Europe and Siberia (Haase et al. 2007; Zykina and Zykina 2008; Haesaerts et al. 2010; Marković et al. 2011). Typically, LPS studies focus on malacology, grain size analyses, magnetic susceptibility, paleopedology and geochemistry, but there is also great potential for developing and applying novel biomarker and compound-specific isotope proxies (Liu and Huang 2005; Zech et al. 2011b; Gao et al. 2012; Zech et al. 2013a, 2013b; Lu et al. 2016). Attempts are increasingly made to establish high-resolution records from LPS and to correlate these with ice core records (Antoine et al. 2009; Kadereit et al. 2013; Heiri et al. 2014). Key to such attempts and for paleoenvironmental reconstructions in general is robust age control.

Chronologies for LPS are typically established by analyzing the stratigraphy, luminescence dating the loess and radiocarbon (<sup>14</sup>C) analyses on charcoal, macrofossils, and soil organic

---

\*Corresponding author: mischa.haas@eawag.ch

carbon from the paleosols (Lang et al. 2003; Frechen et al. 2005; Haesaerts et al. 2010; Stevens et al. 2011). However, uncertainties of luminescence dating are on the order of ~10% for the last glacial cycle, and organic material suitable for  $^{14}\text{C}$  dating is often scarce. This limits the possibility to fully exploit the potential of LPS for paleoclimate and environmental studies, and has motivated research to find alternative ways to date LPS.

Various chemical treatments, such as acid-base-acid (ABA) or acid-base wet oxidation (ABOX), have been suggested to extract soil organic matter fractions that are more reliable for  $^{14}\text{C}$  dating (Hatté et al. 2001a, 2001b). Yet the exact molecular composition of these chemical fractions remains unclear, and in many cases is likely to be heterogeneous in source and age. Roots, microorganisms, and dissolved organic matter might contribute too-young carbon (Matsumoto et al. 2007; Gocke et al. 2014b), whereas more recalcitrant compounds (humins e.g., pyrogenic carbon residues) might be reworked and redeposited, and therefore too old.

A recent study has shown that compound-specific  $^{14}\text{C}$  analyses of long-chain *n*-alkanes and *n*-alkanoic acids yield ages consistent with independent age control based on stratigraphy and luminescence dating (Häggi et al. 2014). Long-chain *n*-alkanes and *n*-alkanoic acids are leaf waxes produced predominantly by higher terrestrial plants, and due to their low water-solubility, chemical inertness and resistance against biodegradation, they are preserved as biomarkers, i.e. molecular fossils, in soils and sediments (Huang et al. 1999; Eglinton and Eglinton 2008).

Within the last 2 decades, compound-specific  $^{14}\text{C}$  analysis has become feasible (Eglinton et al. 1996) and is now more routine. This is technically possible through the development of the mini carbon-dating system MICADAS, an accelerator mass spectrometer (AMS) system that enables on-line coupling of  $\text{CO}_2$ -producing devices (e.g., an elemental analyzer, EA) to gas-accepting ion sources that allow automated measurement of samples containing less than 100  $\mu\text{g}$  carbon (C) (Synal et al. 2007; Ruff et al. 2010; Wacker et al. 2013). A major disadvantage of compound-specific  $^{14}\text{C}$  analyses, however, is the need for a preparative gas chromatography system (Prep-GC) and the very time-consuming laboratory and instrumental procedures to isolate specific compounds in sufficient quantity for AMS analysis. In addition, recoveries are also often very low, which further limits respective applications to samples with sufficiently high concentrations of target analytes.

Due to various practical constraints, we performed this study to empirically test the potential of dating *n*-alkanes as a whole compound class. This approach was previously shown to have promise for  $^{14}\text{C}$  dating of soils (Huang et al. 1999) but had not been applied to LPS. We selected 13 samples from the key LPS Kurtak in central Siberia, spanning from the MIS 3 paleosol through the last glacial loess to the Holocene, and compared the  $^{14}\text{C}$  ages of the extracted and purified *n*-alkanes with independent published age control based on luminescence and  $^{14}\text{C}$  analyses on charcoal and macrofossils.

## **MATERIAL AND METHODS**

### **Geographical Setting and Sampling**

Extensive loess deposits occur in tectonic depressions of the central Siberian platform and on the piedmont plains north of the Altai and Sayan Mountains (Figure 1A, Chlachula 2001; Zykina and Zykina 2008). During cold Pleistocene periods, the region became a prominent periglacial sedimentation area for loess derived from the glacier forefields and river floodplains. The investigated LPS is exposed along the northwestern shore of the Yenisei water reservoir in the Minusinsk Basin near the village of Kurtak (Figure 1B, 55°8'47.472"N, 91°33'25.3074"E).

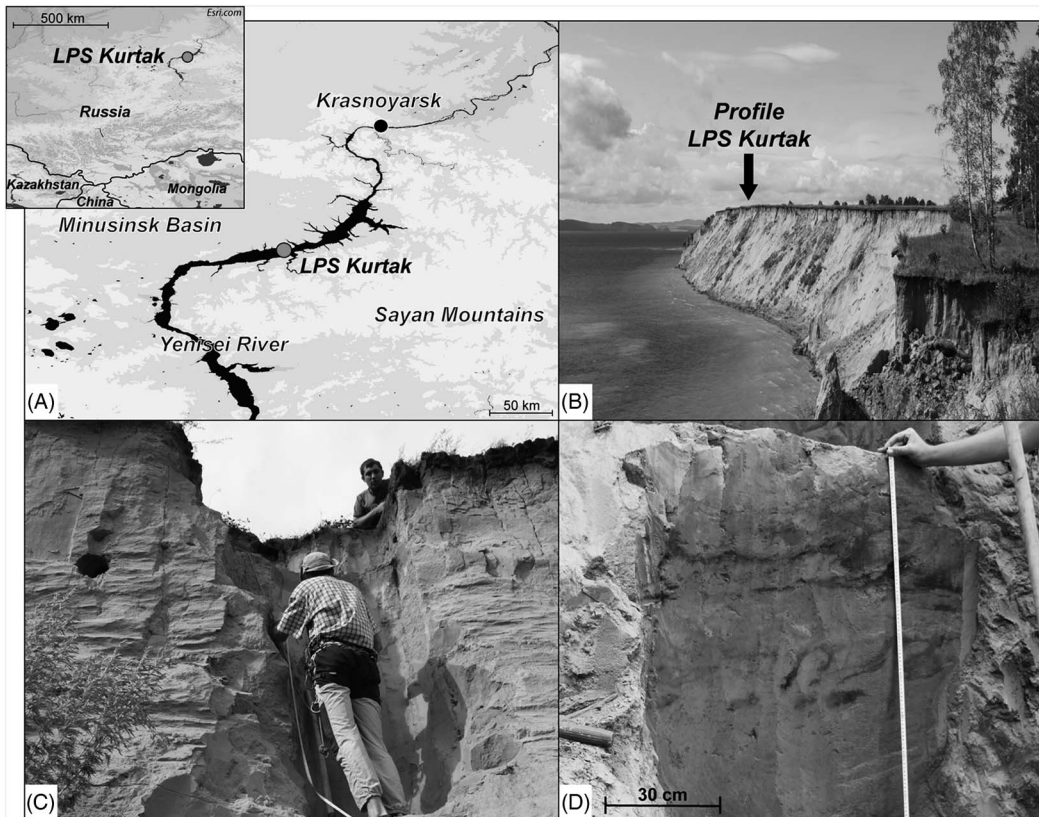


Figure 1 (A) Location of the LPS Kurtak. (B) Picture of the LPS Kurtak. Arrow indicates sampling site. (C) Upper part of LPS Kurtak. (D) Close-up view of the lowermost MIS3 humic-rich layer with cryoturbation structures.

Several studies have focused on the LPS Kurtak in the past, including stratigraphical, paleopedological, archeological, and paleontological research, as well as dating campaigns using luminescence and  $^{14}\text{C}$  analyses (Damblon et al. 1996; Chlachula 2001; Zander et al. 2003; Frechen et al. 2005; Haesaerts et al. 2005). The Holocene soil is a degraded Chernozem typical for the forest-steppe zone in the area, which is intensively used for agriculture. The sampling site was likely used for mowing in the recent past, while birch and pine forests are found nearby, like in many places in the Minusinsk Basin. The topsoil is a ~20 cm Ah-horizon, followed by a ~20 cm thick carbonate free AB-horizon and then a carbonate-rich C-horizon (see Figure 2 left, for a schematic sketch, and Frechen et al. (2005) for a detailed paleopedological description). Modern roots were observed to a depth of ~1 m. The loess, loam and loess-like sediments beneath the Holocene soil (down to ~9 m depth) have accumulated in a tundra and cold steppe environment during the last glaciation, also known as *Sartan glaciation*, correlating with marine isotope stage (MIS) 2 (Arkhipov 1998; Zykina 1999). From 9 m to 11.9 m the “Kurtak Paleosol” documents forest steppe environment during the last interstadial, the *Karginian interstadial* (MIS 3). It is composed of chernozem-like paleosols and several humic-rich layers containing pieces of charcoal, as well as reworked loess in between. The Kurtak Paleosol has been severely affected by cryoturbation (Figure 1D). Below 12 m depth, loess and loess-like sediments document the tundra and cold steppe environment of the MIS 4 glacial period, or *Ermakovo Glaciation* in the north Siberian stratigraphy (Zykina 1999).

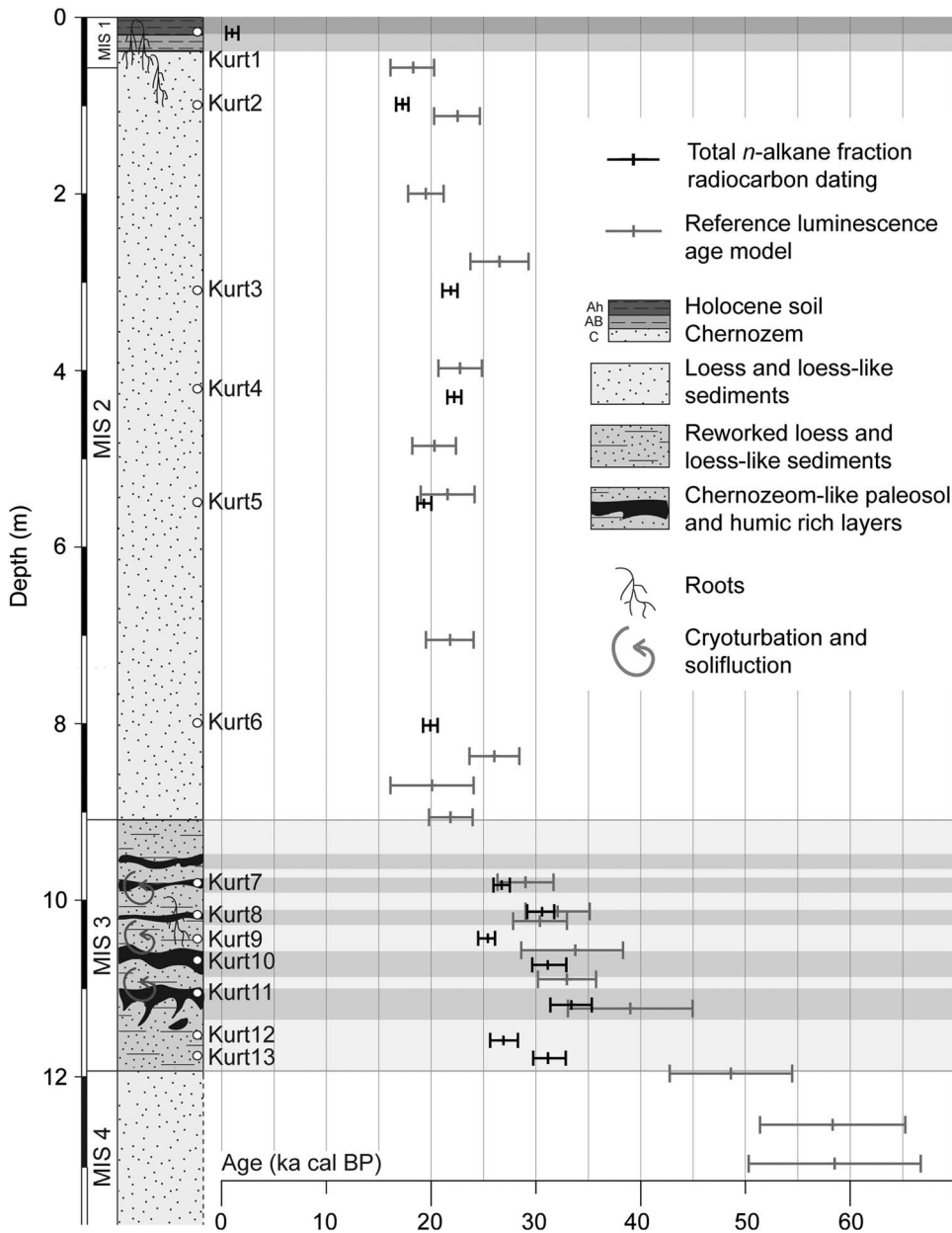


Figure 2 *n*-Alkane age model for the LPS Kurtak (black data points) in correlation and comparison to the luminescence chronology from Zander et al. (2003) and Frechen et al. (2005) (gray data points). The depths of the luminescence samples were adjusted (linearly stretched) to our profile, using the lower and upper boundary of the Kurtak paleosol as tie points.

Fieldwork and sampling was performed in summer 2014. A 1-m-wide and 12-m-high profile was prepared by removing several decimeters from the surface of the steep outcrop (Figure 1C). Samples of 100–150 g each were collected for <sup>14</sup>C dating, one from 20 cm depth (Kurt1), five from the MIS 2 loess unit (Kurt2 to Kurt6), and seven from the MIS 3 Kurtak Paleosol (Kurt7 to Kurt13).

## Sample Preparation and Analyses

The samples were air-dried and homogenized. Aliquots of ~40 g were extracted with dichloromethane and methanol (DCM:MeOH 9:1, all solvents were HPLC grade from Fischer Scientific) using the Dionex ASE 200 accelerated solvent extractor (1000 psi and 100°C, three 15-min cycles) at the Geographical Institute of the University of Bern. Resulting total lipid extracts were separated over aminopropyl columns, with the apolar fractions, containing *n*-alkanes, eluted using *n*-hexane. A gas chromatograph (Agilent 7890) mass spectrometer (Agilent 5975), equipped with an Agilent HP5MS column (30 m × 250 μm × 0.25 μm film thickness), was used for *n*-alkane quantification and identification. 5α-Androstane was used as internal standard and a *n*C<sub>21-40</sub> alkane mixture as external standard. For further purification, samples were passed over AgNO<sub>3</sub> and zeolite (Geokleen 5A, GHGeochemical Services) pipette columns with *n*-hexane. Zeolite is a molecular sieve that traps *n*-alkyl (straight-chain) compounds in its pores. The *n*-alkanes were recovered after drying in an oven (12 hr, 40°C) and dissolving the zeolite in hydrofluoric acid (40%), using liquid-liquid extraction with *n*-hexane. The AgNO<sub>3</sub>-zeolite *n*-alkane cleanup recoveries were ~80–90%. After again checking the *n*-alkanes for purity by GC-MS, aliquots were transferred with DCM into tin capsules (sample vessels from Elementar, Art. Nr. 05001727, 3.5 × 5.5 × 0.1 mm), and the DCM was evaporated on a hotplate at 35°C.

<sup>14</sup>C measurements were performed on a MICADAS AMS coupled online to an EA unit (Vario MICRO cube from Elementar, Synal et al. 2007; Ruff et al. 2010; Wacker et al. 2013; Salazar et al. 2015) at the LARA AMS Laboratory, University of Bern (Szidat et al. 2014). Results are reported as fraction modern (F<sup>14</sup>C), normalized using the reference material Oxalic Acid II (National Institute of Standards and Technology) after subtracting the background signal (Wacker et al. 2010). Sodium acetate (n = 6) with a F<sup>14</sup>C of 0.013 ± 0.001 was used as fossil standard in order to estimate the background signal.

All <sup>14</sup>C measurements were corrected using the contamination drift model presented by Salazar et al. (2015). It assumes a combination of constant blank contamination (mass *m<sub>c</sub>* and <sup>14</sup>C/<sup>12</sup>C ratio *R<sub>c</sub>*) and cross contamination. In order to quantify and correct for constant contamination, we repeatedly measured 10 combined tin capsules. A single capsule yielded on average 0.43 ± 0.11 μg C for *m<sub>c</sub>* with a F<sup>14</sup>C of 0.76 ± 0.18. For error propagation, we assumed constant contamination and uncertainties of 15% and 20% for blank mass and F<sup>14</sup>C, respectively (Salazar et al. 2015). A cross contamination of 0.2 ± 0.1 % from the previous sample was determined for the EA-AMS system and was also corrected for following Salazar et al. (2015), including full error propagation.

Calibrated <sup>14</sup>C ages were calculated using OxCal (Bronk Ramsey 2009) and the IntCal13 calibration curve (Reimer et al. 2013). The calendar ages in this study are reported as calibrated ages before present (cal BP) and as age intervals in the 2σ probability range (95.4%).

## RESULTS

Long-chain *n*-alkane concentrations (ΣC<sub>25</sub>-C<sub>35</sub>) in our samples range from 0.6 to 7.6 μg/g dry sediment. These homologues are the most abundant ones, typify vascular plant leaf cuticular wax *n*-alkanes, and we herein refer to them as “leaf wax” *n*-alkanes. Leaf wax *n*-alkane concentrations are lowest in the MIS 2 loess (0.6–1.2 μg/g), whereas the Holocene sample Kurt1 has a concentration of 1.9 μg/g, and concentrations are as high as 7.6 μg/g in the Kurtak paleosol.

Carbon amounts analyzed for purified *n*-alkane fractions on the EA-AMS ranged from 17.3 to 113.8 μg C (Table 1). F<sup>14</sup>C for *n*-alkanes from sample Kurt1 at 20 cm depth is 0.865 ± 0.032 and

Table 1  $^{14}\text{C}$  analysis of *n*-alkane fractions in stratigraphic order.

Sample	BE nr	Depth (m)	$\mu\text{g C}^{\text{a}}$	$\text{F}^{14}\text{C}$	Uncertainty (%)	Calibrated age intervals ( $2\sigma$ )			
						From (cal BP)	To (cal BP)	Probability (%)	Median calendar age (cal BP)
Kurt1	3609.1.1	0.2	57.1	0.865	0.032	632 560	1702 598	94.5 0.9	1104
Kurt2	3610.1.1	1.0	28.1	0.170	0.004	16,701	17,868	95.4	17,298
Kurt3	3611.1.1	3.1	26.4	0.105	0.004	21,089	22,521	95.4	21,885
Kurt4	3612.1.1	4.3	34.0	0.102	0.004	21,561	22,890	95.4	22,216
Kurt5	3613.1.1	5.5	17.3	0.136	0.005	18,715	20,038	95.4	19,328
Kurt6	3614.1.1	8.0	22.9	0.128	0.004	19,246	20,631	95.4	19,945
Kurt7	3619.1.1	9.8	38.6	0.061	0.003	25,944	27,489	95.4	26,719
Kurt8	3616.1.1	10.1	56.2	0.037	0.003	29,146	31,708	95.4	30,559
Kurt9	3620.1.1	10.4	38.5	0.072	0.003	24,485	26,085	95.4	25,403
Kurt10	3621.1.1	10.7	81.6	0.035	0.003	29,632	32,861	95.4	31,105
Kurt11	3622.1.1	11.15	113.8	0.026	0.003	31,350	35,280	95.4	33,350
Kurt12	3617.1.1	11.55	33.5	0.060	0.005	25,630	28,271	95.4	26,885
Kurt13	3618.1.1	11.75	68.2	0.035	0.003	29,716	32,806	95.4	31,120

<sup>a</sup>Quantity of combusted and injected carbon, measured by the EA unit.

yields a calibrated  $^{14}\text{C}$  age interval of 0.6–1.7 ka cal BP. Samples from the underlying loess (Kurt2 to Kurt6) have  $\text{F}^{14}\text{C}$  values from 0.170 to 0.102 and calibrated ages range from 16.7 to 22.9 ka cal BP. Within uncertainties, they seem stratigraphically consistent and document rapid loess accumulation during MIS 2 at ~22 ka BP. The samples Kurt7 to Kurt13 from the Kurtak Paleosol have  $\text{F}^{14}\text{C}$  values from 0.072 to 0.026 and ages from 24.5 to 35.3 ka cal BP. They are all older than the samples from the overlying loess, but not stratigraphically consistent when compared to each other. This may reflect the fact that the Kurtak Paleosol is strongly cryoturbated, but this interpretation requires further assessment.

## DISCUSSION

### Comparison with Independent Age Control

The  $^{14}\text{C}$  ages of *n*-alkanes from the Kurtak LPS are in very good agreement with independent age control for the Kurtak LPS based on stratigraphy, luminescence, and  $^{14}\text{C}$  dating on charcoal and macrofossils. Zander et al. (2003) and Frechen et al. (2005) reported IRSL luminescence ages for the MIS 2 loess ranging from  $17.9 \pm 2.1$  to  $26.3 \pm 2.8$  ka (Figure 2). Within uncertainties, the luminescence ages are stratigraphically consistent and have been interpreted to document rapid loess accumulation at ~22 ky. Note that our Kurt1 sample from 20 cm depth is 0.6–1.7 ka cal BP and reflects recent pedogenesis, whereas our Kurt2 sample from 1 m depth is 16.7–17.9 ka cal BP and in good agreement with the IRSL age of  $17.9 \pm 2.1$  ka at ~70 cm depth.

For the Kurtak Paleosol, Zander et al. (2003) and Frechen et al. (2005) reported IRSL ages ranging from  $28.8 \pm 2.7$  to  $36.0 \pm 3.2$  ka. Damblon et al. (1996) and Haesaerts et al. (2005, 2014) reported dozens of  $^{14}\text{C}$  ages from charcoal and wood remains, which were deposited in a topographic depression in a nearby section. Uncalibrated ages range from  $25.7 \pm 0.5$  to  $42.5 \pm 0.7$  ka BP. Calibration yields ages from 29.7 to 47.4 ka cal BP, so within uncertainties our leaf wax *n*-alkane  $^{14}\text{C}$  ages for the Kurtak Paleosol (ranging from 24.5 to 35.3 ka cal BP) are in good agreement with reported luminescence and  $^{14}\text{C}$  ages. All findings corroborate that the Kurtak Paleosol formed during MIS 3. The underlying MIS 4 loess yields IRSL ages of ~60 ka (Figure 2, Zander et al. 2003; Frechen et al. 2005), which is beyond the reach of  $^{14}\text{C}$  dating.

### Analytical Uncertainties

The assumed constant contamination, which we determined by combining 10 empty tin capsules and for which we corrected all our <sup>14</sup>C measurements, was 0.43 μg C. This value is almost identical to the value of 0.4 μg C reported for tin capsules by Ruff et al. (2010), yet lower compared to a vacuum line blank of 0.91 μg C reported by Häggi et al. (2014) and a full process blank of 1 μg C reported by Shah and Pearson (2007). Our F<sup>14</sup>C value for the assumed constant contamination is 0.76, which is in agreement with 0.65 determined by Ruff et al. (2010), but higher than F<sup>14</sup>C values of 0.23 and 0.2 reported by Häggi et al. (2014) and Shah and Pearson (2007), respectively.

Future work should aim at searching for capsules with lower F<sup>14</sup>C and amount of carbon, in order to reduce uncertainties propagated to glacial and deglacial age samples. In this study, our corrections for constant contamination were between 0 and 0.01 F<sup>14</sup>C for all samples, with the Kurt5 subject to the largest correction (0.01 F<sup>14</sup>C), as it contained only 17.3 μg C. Corrections for cross contamination are negligible (<< 0.01 F<sup>14</sup>C) because samples with similar <sup>14</sup>C were measured consecutively.

With regard to current analytical uncertainties, we note that (1) large sample sizes are essential to minimize uncertainties, especially for old samples (>20 ka BP) that contain low <sup>14</sup>C abundances; (2) the <sup>14</sup>C age scatter in the Kurtak Paleosol (MIS 3) exceeds the estimated analytical uncertainties and likely reflects the massive cryoturbation observed in the field; and (3) given sufficient sample availability, leaf waxes can be dated with reasonable uncertainties back to ~35–40 ka BP, corresponding to ~0.02 F<sup>14</sup>C.

### Contributions from Fossil or Post-Sedimentary Lipids?

The *n*-alkane homologue patterns of all investigated samples show a strong dominance of odd, long-chain (C<sub>25</sub> to C<sub>35</sub>) *n*-alkanes (Figure 3). This is typical for epicuticular leaf waxes of higher terrestrial plants (Eglinton and Hamilton 1967; Eglinton and Eglinton 2008). C<sub>31</sub> is the most abundant homologue for all samples with the exception of Kurt2 (C<sub>max</sub> = C<sub>29</sub>). This, as well as relatively long average chain lengths (abundance-weighted average of C<sub>25</sub>, C<sub>27</sub>, C<sub>29</sub>, C<sub>31</sub>, C<sub>33</sub>, and C<sub>35</sub>) from 30.2 to 31.2 for the samples Kurt3 to Kurt13, points to grasses and herbs as dominant sources for the leaf waxes (Schäfer et al. 2016 and references therein). Only the C<sub>29</sub> dominance of Kurt2 and relatively short average chain lengths of 29.9 and 29.8 for Kurt1 and Kurt2, respectively, indicate some additional leaf wax input from deciduous trees and shrubs (Schäfer et al. 2016).

Odd-over-even chain length predominances (OEP), calculated as ratios of C<sub>27</sub>, C<sub>29</sub>, C<sub>31</sub>, and C<sub>33</sub> over C<sub>26</sub>, C<sub>28</sub>, C<sub>30</sub>, and C<sub>32</sub>, following Hoefs et al. (2002) and Schäfer et al. (2016), range from 6.2 to 20.6, indicating good preservation of the leaf waxes and little degradation. Low OEPs (~1) and occurrence of shorter chains (<C<sub>25</sub>) would point to possible input from reworked fossil *n*-alkanes and yield stratigraphically inconsistent and too old <sup>14</sup>C ages (Lichtfouse et al. 1997; Häggi et al. 2014).

We conclude that reworked leaf waxes, or fossil *n*-alkanes are unlikely to have contributed significantly to the sedimentary *n*-alkane signatures in the LPS Kurtak. Nevertheless, when compound-specific <sup>14</sup>C dating is an option, we recommend determining <sup>14</sup>C ages for odd and even *n*-alkanes separately, as discrepancies between these homologues could reveal fossil inputs (Häggi et al. 2014).

It is important to note that reworking associated with eolian processes may contribute not only fossil organic material, but also contemporary, non-local leaf waxes. Wind abrasion and

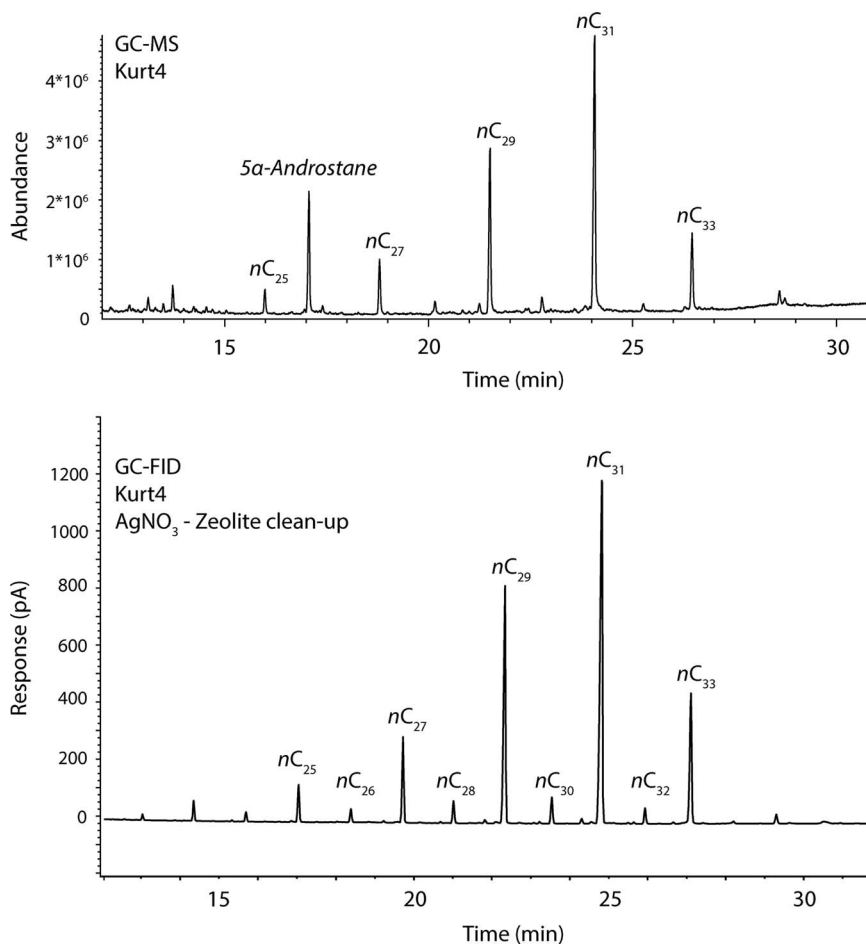


Figure 3 *n*-Alkane homologue pattern of sample Kurt4 before and after the AgNO<sub>3</sub>-Zeolite purification.

sandblasting of leaf surfaces can produce airborne wax *n*-alkanes, which are transported and deposited in adjacent regions (Conte et al. 2003). Leaf wax homologue patterns and compound-specific stable isotope signals might thus be biased by the dust/leaf wax source region. Little is presently known concerning the relevance of such biases. More importantly, however, non-local leaf waxes will not influence the <sup>14</sup>C signal of leaf waxes in LPS provided that they are produced and deposited contemporaneously. Eolian transport of leaf waxes does therefore not limit their potential for <sup>14</sup>C dating LPS.

Post-sedimentary biogenic lipid contributions formed or introduced at depth would, on the other hand, result in too young <sup>14</sup>C ages. It has been suggested that roots and rhizomicrobial activity are a significant source of long-chain *n*-alkyl lipids in the subsurface and may affect paleoenvironmental reconstructions based on leaf waxes in LPS. Root tissues tend to contain more C<sub>25</sub> and C<sub>27</sub> *n*-alkanes than longer-chain homologues (Gocke et al. 2014a) or are dominated by short-chain homologues (< C<sub>25</sub>) (Kirkels et al. 2013). Litterbag studies document that microbial activity leads to post-sedimentary alteration of leaf wax patterns and corresponding isotopic compositions during early degradation (Nguyen Tu et al. 2011; Zech et al. 2011a).

Matsumoto et al. (2007) performed compound-specific <sup>14</sup>C dating on *n*-alkanoic acids in soils and suggested that the systematically younger ages for C<sub>24</sub> and C<sub>26</sub> compared to longer homologues can be explained with higher solubility and leaching, as well as with preferential microbial degradation and production. Häggi et al. (2014) also found a tendency of younger ages for shorter-chain *n*-alkanoic acids and *n*-alkanes in four samples from the LPS Crvenka in Serbia, yet the overall good consistency of their <sup>14</sup>C ages with the stratigraphy and independent age control based on luminescence led them to conclude that post-sedimentary lipid contributions at great depth were negligible. Likewise, we argue that the overall good agreement of our <sup>14</sup>C ages with stratigraphy, luminescence and <sup>14</sup>C dating, particularly in the MIS 2 loess, indicates that post-sedimentary contributions of long-chain *n*-alkanes are insignificant.

While we cannot fully exclude the possibility that post-sedimentary lipids, e.g. related to rhizomicrobial activity, were produced in the Kurtak Paleosol and cause slightly too-young and stratigraphically inconsistent ages (Kurt9 and 12, ~26 ka cal BP), we argue that these ages make perfect sense in view of the evidence for strong cryoturbation. Both these samples (Kurt9 and 12) are from reworked loess low in organic matter (see Figure 2), whereas the organic-rich samples (e.g. Kurt8, 10 and 11) are slightly older (~30–35 ka cal BP) and more consistent with the luminescence ages. We suggest that humus accumulation occurred before ~30 ka, i.e. during MIS 3, and that strong cryoturbation, solifluction and loess accumulation began with the transition into MIS 2. Thus, periglacial cover beds, dominated by organic-rich, reworked MIS 3 paleosols yield MIS 3 ages, whereas cover beds dominated by MIS 2 loess yield slightly younger MIS 2 ages.

## CONCLUSIONS

<sup>14</sup>C dating of leaf wax *n*-alkane fractions in the LPS Kurtak resulted in good agreement (i.e., within methodological uncertainties) with independent, published ages of this sequence based on stratigraphy, luminescence, and <sup>14</sup>C dating of charcoal and macrofossils. The uppermost Holocene sample reflects ongoing pedogenesis as well as humus accumulation. The samples from the underlying MIS 2 sediments document rapid loess accumulation at ~22 ka BP. The Kurtak Paleosol *n*-alkanes yielded <sup>14</sup>C ages between 24.5 and 35.3 ka cal BP and are in good agreement with independent age control. The Kurtak Paleosol formed during MIS 3, but we suggest that strong cryoturbation and solifluction early during MIS 2 affected this paleosol and explains the observed age inversions and some apparently too-young <sup>14</sup>C ages. Methodological artifacts, related to rhizomicrobial activity or analytical uncertainties, are probably much less relevant. The current analytical limits are estimated to be ~35–40 ka BP, corresponding to ~0.02 F<sup>14</sup>C.

Overall, our findings corroborate the stratigraphic integrity of leaf waxes in LPS and underline their potential as an innovative tool for <sup>14</sup>C dating, particularly when charcoal and macrofossils are not available. Contributions from reworked *n*-alkanes (fossil hydrocarbons), which would result in too-old <sup>14</sup>C ages, or from post-depositional processes (roots and rhizomicrobial activity), which would result in too-young ages, are negligible.

Separation and purification of long-chain *n*-alkanes over AgNO<sub>3</sub> and zeolite pipette columns is relatively quick and easy, and recoveries are high, paving the way for rapid compound class-level <sup>14</sup>C dating. The scope of this approach could be further extended by (1) extracting large sample amounts to minimize blank corrections, and (2) limiting sample batches to “very low <sup>14</sup>C” samples in order to minimize cross contamination. <sup>14</sup>C dating of leaf wax *n*-alkanes as a compound class represents a promising method for developing LPS chronologies. Future studies could be extended to long-chain *n*-alkanoic acids, or other leaf wax compound classes.

## ACKNOWLEDGMENTS

We would like to thank PD Dr. Michael Zech (University of Dresden) for his support during the concept development for this study, Imke Schäfer for her help in the field, and Lorenz Wüthrich for his support during sample preparation in the laboratory. We also thank the SNSF for funding (PP00P2 150590).

## REFERENCES

- Antoine P, Rousseau D-D, Moine O, Kunesch S, Hatte C, Lang A, Tissoux H, Zöller L. 2009. Rapid and cyclic aeolian deposition during the Last Glacial in European loess: a high-resolution record from Nussloch, Germany. *Quaternary Science Reviews* 28(25):2955–73.
- Arkipov S. 1998. Stratigraphy and paleogeography of the Sartan glaciation in west Siberia. *Quaternary International* 45:29–42.
- Bradley RS. 1999. *Paleoclimatology: Reconstructing Climates of the Quaternary*. Academic Press.
- Bronk Ramsey C. 2009. Bayesian analysis of radiocarbon dates. *Radiocarbon* 51(1):337–60.
- Chlachula J. 2001. Pleistocene climate change, natural environments and palaeolithic occupation of the upper Yenisei area, south-central Siberia. *Quaternary International* 80:101–30.
- Conte MH, Weber JC, Carlson PJ, Flanagan LB. 2003. Molecular and carbon isotopic composition of leaf wax in vegetation and aerosols in a northern prairie ecosystem. *Oecologia* 135(1):67–77.
- Damblon F, Haesaerts P, van der Plicht J. 1996. New datings and considerations on the chronology of Upper Palaeolithic sites in the Great Eurasian Plain. *Préhistoire européenne* 9: 177–231.
- Derbyshire E, Kemp RA, Meng X. 1997. Climate change, loess and palaeosols: proxy measures and resolution in North China. *Journal of the Geological Society* 154(5):793–805.
- Eglinton G, Hamilton RJ. 1967. Leaf epicuticular waxes. *Science* 156(3780):1322–35.
- Eglinton TI, Aluwihare LI, Bauer JE, Druffel ER, McNichol AP. 1996. Gas chromatographic isolation of individual compounds from complex matrices for radiocarbon dating. *Analytical Chemistry* 68(5):904–12.
- Eglinton TI, Eglinton G. 2008. Molecular proxies for paleoclimatology. *Earth and Planetary Science Letters* 275(1):1–16.
- Field C, Van Aalst M. 2014. *Climate Change 2014: Impacts, Adaptation, and Vulnerability*. IPCC.
- Frechen M, Zander A, Zykina V, Boenigk W. 2005. The loess record from the section at Kurtak in Middle Siberia. *Palaeogeography, Palaeoclimatology, Palaeoecology* 228(3):228–44.
- Gao L, Nie J, Clemens S, Liu W, Sun J, Zech R, Huang Y. 2012. The importance of solar insolation on the temperature variations for the past 110kyr on the Chinese Loess Plateau. *Palaeogeography, Palaeoclimatology, Palaeoecology* 317:128–33.
- Gocke M, Gulyás S, Hambach U, Jovanović M, Kovács G, Marković SB, Wiesenberg GL. 2014a. Biopores and root features as new tools for improving paleoecological understanding of terrestrial sediment-paleosol sequences. *Palaeogeography, Palaeoclimatology, Palaeoecology* 394: 42–58.
- Gocke M, Peth S, Wiesenberg GL. 2014b. Lateral and depth variation of loess organic matter overprint related to rhizoliths—revealed by lipid molecular proxies and X-ray tomography. *Catena* 112:72–85.
- Haase D, Fink J, Haase G, Ruske R, Pecs M, Richter H, Altermann M, Jäger K-D. 2007. Loess in Europe – its spatial distribution based on a European Loess Map, scale 1: 2,500,000. *Quaternary Science Reviews* 26(9):1301–12.
- Haesaerts P, Chekha VP, Damblon F, Drozdov NI, Orlova LA, van der Plicht J. 2005. The loess-palaeosol succession of Kurtak (Yenisei basin, Siberia): a reference record for the Karga stage (MIS 3). *Revue de l'Association française pour l'étude du Quaternaire* 16(1):3–24.
- Haesaerts P, Borziac I, Chekha V, Chirica V, Drozdov N, Koulakovska L, Orlova L, van der Plicht J, Damblon F. 2010. Charcoal and wood remains for radiocarbon dating Upper Pleistocene loess sequences in Eastern Europe and Central Siberia. *Palaeogeography, Palaeoclimatology, Palaeoecology* 291(1):106–27.
- Haesaerts P, Damblon F, Drozdov N, Chekha V, van der Plicht J. 2014. Variability in Radiocarbon Dates in Middle Pleniglacial Wood from Kurtak (Central Siberia). *Radiocarbon* 56(3):1195–206.
- Häggi C, Zech R, McIntyre C, Zech M, Eglinton T. 2014. On the stratigraphic integrity of leaf-wax biomarkers in loess paleosols. *Biogeosciences* 11(9): 2455–63.
- Hatté C, Pessenda LC, Lang A, Paterne M. 2001a. Development of Accurate and Reliable <sup>14</sup>C Chronologies for Loess Deposits: Application to the Loess Sequence of Nussloch (Rhine Valley, Germany). *Radiocarbon* 43(2):611–8.
- Hatté C, Morvan J, Noury C, Paterne M. 2001b. Is classical acid-alkali-acid treatment responsible for contamination? An alternative proposition. *Radiocarbon* 43(2A):177–82.
- Heiri O, Koinig KA, Spötl C, Barrett S, Brauer A, Drescher-Schneider R, Gaar D, Ivy-Ochs S, Kerschner H, Luetscher M. 2014. Palaeoclimate records 60–8 ka in the Austrian and Swiss Alps and their forelands. *Quaternary Science Reviews* 106:186–205.

- Hoefs MJ, Rijpstra WIC, Damsté JSS. 2002. The influence of oxic degradation on the sedimentary biomarker record I: evidence from Madeira Abyssal Plain turbidites. *Geochimica et Cosmochimica Acta* 66(15):2719–35.
- Huang Y, Li B, Bryant C, Bol R, Eglinton G. 1999. Radiocarbon dating of aliphatic hydrocarbons a new approach for dating passive-fraction carbon in soil horizons. *Soil Science Society of America Journal* 63(5):1181–7.
- Kadereit A, Kind C-J, Wagner GA. 2013. The chronological position of the Lohne Soil in the Nussloch loess section—reevaluation for a European loess-marker horizon. *Quaternary Science Reviews* 59:67–86.
- Kirkels FM, Jansen B, Kalbitz K. 2013. Consistency of plant-specific n-alkane patterns in plaggen ecosystems: a review. *The Holocene* 23(9):1355–68.
- Kukla G. 1987. Loess stratigraphy in central China. *Quaternary Science Reviews* 6(3):191–219.
- Lang A, Hatté C, Rousseau D-D, Antoine P, Fontugne M, Zöller L, Hambach U. 2003. High-resolution chronologies for loess: comparing AMS  $^{14}\text{C}$  and optical dating results. *Quaternary Science Reviews* 22(10):953–9.
- Lichtfouse E, Budzinski H, Garrigues P, Eglinton TI. 1997. Ancient polycyclic aromatic hydrocarbons in modern soils:  $^{13}\text{C}$ ,  $^{14}\text{C}$  and biomarker evidence. *Organic Geochemistry* 26(5):353–9.
- Liu W, Huang Y. 2005. Compound specific D/H ratios and molecular distributions of higher plant leaf waxes as novel paleoenvironmental indicators in the Chinese Loess Plateau. *Organic Geochemistry* 36(6):851–60.
- Lu H, Liu W, Wang H, Wang Z. 2016. Variation in 6-methyl branched glycerol dialkyl glycerol tetraethers in Lantian loess–paleosol sequence and effect on paleotemperature reconstruction. *Organic Geochemistry* 100:10–7.
- Marković SB, Hambach U, Stevens T, Kukla GJ, Heller F, McCoy WD, Oches EA, Bugge B, Zöller L. 2011. The last million years recorded at the Stari Slankamen (Northern Serbia) loess-paleosol sequence: revised chronostratigraphy and long-term environmental trends. *Quaternary Science Reviews* 30(9):1142–54.
- Matsumoto K, Kawamura K, Uchida M, Shibata Y. 2007. Radiocarbon content and stable carbon isotopic ratios of individual fatty acids in subsurface soil: implication for selective microbial degradation and modification of soil organic matter. *Geochemical Journal* 41(6):483–92.
- Nguyen Tu TT, Egasse C, Zeller B, Bardoux G, Biron P, Ponge J-F, David B, Derenne S. 2011. Early degradation of plant alkanes in soils: A litterbag experiment using  $^{13}\text{C}$ -labelled leaves. *Soil Biology and Biochemistry* 43(11):2222–8.
- Pécsi M. 1990. Loess is not just the accumulation of dust. *Quaternary International* 7:1–21.
- Reimer PJ, Bard E, Bayliss A, Beck JW, Blackwell PG, Bronk Ramsey C, Buck CE, Cheng H, Edwards RL, Friedrich M, Grootes PM, Guilderson TP, Hafidason H, Hajdas I, Hatté C, Heaton TJ, Hoffmann DL, Hogg AG, Hughen KA, Kaiser KF, Kromer B, Manning SW, Niu M, Reimer RW, Richards DA, Scott EM, Southon JR, Staff RA, Turney CSM, van der Plicht J. 2013. IntCal13 and Marine13 radiocarbon age calibration curves 0–50,000 years cal BP. *Radiocarbon* 55(4):1869–87.
- Ruff M, Fahrni S, Gägger H, Hajdas I, Suter M, Synal H-A, Szidat S, Wacker L. 2010. On-line radiocarbon measurements of small samples using elemental analyzer and MICADAS gas ion source. *Radiocarbon* 52(4):1645–56.
- Salazar G, Zhang Y, Agrios K, Szidat S. 2015. Development of a method for fast and automatic radiocarbon measurement of aerosol samples by online coupling of an elemental analyzer with a MICADAS AMS. *Nuclear Instruments and Methods in Physics Research B* 361:163–7.
- Schäfer I, Lanny V, Franke J, Eglinton TI, Zech M, Vysloužilová B, Zech R. 2016. Leaf waxes in litter and topsoils along a European transect. *SOIL Discuss* 2016:1–18.
- Shah SR, Pearson A. 2007. Ultra-Microscale (5–25  $\mu\text{g}$  C) Analysis of individual lipids by  $^{14}\text{C}$  AMS: assessment and correction for sample processing blanks. *Radiocarbon* 49(1):69.
- Stevens T, Marković SB, Zech M, Hambach U, Sümeği P. 2011. Dust deposition and climate in the Carpathian Basin over an independently dated last glacial–interglacial cycle. *Quaternary Science Reviews* 30(5):662–81.
- Synal H-A, Stocker M, Suter M. 2007. MICADAS: a new compact radiocarbon AMS system. *Nuclear Instruments and Methods in Physics Research B* 259(1):7–13.
- Szidat S, Salazar GA, Vogel E, Battaglia M, Wacker L, Synal H-A, Türlér A. 2014.  $^{14}\text{C}$  analysis and sample preparation at the new Bern Laboratory for the Analysis of Radiocarbon with AMS (LARA). *Radiocarbon* 56(2):561–6.
- Wacker L, Christl M, Synal H-A. 2010. Bats: a new tool for AMS data reduction. *Nuclear Instruments and Methods in Physics Research B* 268(7):976–9.
- Wacker L, Fahrni S, Hajdas I, Molnar M, Synal H-A, Szidat S, Zhang Y. 2013. A versatile gas interface for routine radiocarbon analysis with a gas ion source. *Nuclear Instruments and Methods in Physics Research Section B* 294:315–9.
- Zander A, Frechen M, Zykina V, Boenigk W. 2003. Luminescence chronology of the Upper Pleistocene loess record at Kurtak in Middle Siberia. *Quaternary Science Reviews* 22(10):999–1010.
- Zech M, Pedentchouk N, Bugge B, Leiber K, Kalbitz K, Marković SB, Glaser B. 2011a. Effect of leaf litter degradation and seasonality on D/H isotope ratios of n-alkane biomarkers. *Geochimica et Cosmochimica Acta* 75(17):4917–28.

- Zech M, Zech R, Buggle B, Zöller L. 2011b. Novel methodological approaches in loess research—interrogating biomarkers and compound-specific stable isotopes. *Quaternary Science Journal* 60: 170–87.
- Zech M, Tuthorn M, Detsch F, Rozanski K, Zech R, Zöller L, Zech W, Glaser B. 2013a. A 220ka terrestrial  $\delta^{18}\text{O}$  and deuterium excess biomarker record from an eolian permafrost paleosol sequence, NE-Siberia. *Chemical Geology* 360:220–30.
- Zech R, Zech M, Marković S, Hambach U, Huang Y. 2013b. Humid glacial, arid interglacials? Critical thoughts on pedogenesis and paleoclimate based on multi-proxy analyses of the loess–paleosol sequence Crvenka, Northern Serbia. *Palaeogeography, Palaeoclimatology, Palaeoecology* 387: 165–75.
- Zykina V. 1999. Pleistocene pedogenesis and climate history of western Siberia. *Quaternary of Siberia. Quaternary Geology, Palaeogeography, and Palaeolithic Archaeology, Anthropozoikum* 23: 49–54.
- Zykina V, Zykin V. 2008. The loess–soil sequence of the Brunhes chron from West Siberia and its correlation to global and climate records. *Quaternary International* 179(1):1715.